Hydrol. Earth Syst. Sci. Discuss., 10, 8031–8069, 2013
www.hydrol-earth-syst-sci-discuss.net/10/8031/2013/
doi:10.5194/hessd-10-8031-2013

Hydrology and Earth System Sciences
Open Access
Discussions

Sr isotopic characteristics in two small watersheds draining typical silicate and carbonate rocks: implication for the studies on seawater Sr isotopic evolution

W. H. Wu[1], H. B. Zheng[2], and J. D. Yang[3]

[1]Key Laboratory of Surficial Geochemistry, Ministry of Education;
School of Earth Sciences and Engineering, Nanjing University, Nanjing 210093, China
[2]School of Geography Science, Nanjing Normal University, Nanjing 210046, China
[3]Center of Modern Analysis Nanjing University, Nanjing 210093, China

Received: 30 May 2013 – Accepted: 12 June 2013 – Published: 21 June 2013

Correspondence to: W. H. Wu (wuwh@nju.edu.cn)

Published by Copernicus Publications on behalf of the European Geosciences Union.

Abstract

We systematically investigated Sr isotopic characteristics of small silicate watershed – the tributary Xishui River of the Yangtze River, and small carbonate watershed – the tributary Guijiang River of the Pearl River. The results show that the Xishui River has relatively high Sr concentrations (0.468–1.70 µmol L^{-1} in summer and 1.30–3.17 µmol L^{-1} in winter, respectively) and low $^{87}Sr/^{86}Sr$ ratios (0.708686–0.709148 in summer and 0.708515–0.709305 in winter), which is similar to the characteristics of carbonate weathering. The Guijiang River has low Sr concentrations (0.124–1.098 µmol L^{-1}) and high $^{87}Sr/^{86}Sr$ ratios (0.710558–0.724605), being characterized by silicate weathering.

In the Xishui River catchment, chemical weathering rates in summer are far higher than those in winter, indicating significant influence of climate regime. However, slight differences of $^{87}Sr/^{86}Sr$ ratios between summer and winter show that influence of climate on Sr isotope is uncertainty owing to very similar Sr isotope values in silicate and carbonate bedrocks. As $^{87}Sr/^{86}Sr$ ratios in the Xishui River are lower than those in seawater, they will decrease $^{87}Sr/^{86}Sr$ ratio of seawater after transported into oceans. Previous studies also showed that some basaltic watersheds with extremely high chemical weathering rates reduced the seawater Sr isotope ratios. In other words, river catchments with high silicate weathering rates do not certainly transport highly radiogenic Sr into oceans. Therefore, it may be questionable that using the variations of seawater $^{87}Sr/^{86}Sr$ ratio to indicate the continental silicate weathering intensity.

In the Guijiang River catchment, $^{87}Sr/^{86}Sr$ ratios of carbonate rocks and other sources (rainwater, domestic and industrial waste water, and agricultural fertilizer) are lower than 0.71. In comparison, some non-carbonate components, such as, sand rocks, mud rocks, shales, have relatively high Sr isotopic compositions. Moreover, granites accounted for only 5 % of the drainage area have extremely high $^{87}Sr/^{86}Sr$ ratios with an average of over 0.8. Therefore, a few silicate components contained in carbonate rocks obviously increases the Sr isotopic compositions of the river water, and

results in a positive effect on the rise of $^{87}Sr/^{86}Sr$ ratio of seawater. Therefore, the relation between Sr isotope evolution of seawater and continental weathering rate is complex, $^{87}Sr/^{86}Sr$ ratios of underlying bedrock in catchment could be an important controlling factors.

1 Introduction

By analyzing the Sr isotopic compositions of marine limestones and their shells, evolution curve of seawater $^{87}Sr/^{86}Sr$ in the Phanerozoic was well established (Veizer and Compston, 1974; Brass, 1976; Burke et al., 1982; DePaolo and Ingram, 1985; Palmer and Elderfield, 1985; DePaolo, 1986; Hess et al., 1986; Richter and DePaolo, 1987, 1988; Raymo et al., 1988; Veizer, 1989; Capo and DePaolo, 1990; Hodell et al., 1991; Richter et al., 1992; Veizer et al., 1999; Korte et al., 2006; Melezhik et al., 2009). The Sr isotope budget of the oceans is dominated by its supplies via rivers, hydrothermal vent waters, and diagenesis of deep-sea sediments, and the dissolved Sr flux to the modern oceans via rivers is far more than those via the latter two (Palmer and Edmond, 1989). Particularly, the Ganges and Brahmaputra originating in the southern Qinghai-Tibet Plateau are characterized by both high Sr concentrations and $^{87}Sr/^{86}Sr$ ratios, and so have a major influence on the rise of Sr isotopic composition of seawater (e.g. Krishnaswami et al., 1992; Harris, 1995; Derry and France-Lanord, 1996; Quade et al., 1997; Galy et al., 1999; English et al., 2000; Singh et al., 2006). Therefore, many researchers considered that the steady increase of $^{87}Sr/^{86}Sr$ in the oceans since Cenozoic was mainly attributed to uplifting of the Qinghai-Tibet Plateau, which caused increased silicate weathering and highly radiogenic Sr flux to oceans. As the silicate rocks in the south Himalaya have both high $^{87}Sr/^{86}Sr$ ratios and high Sr concentrations, the rise of Sr isotopic composition of seawater since Cenozoic can be used as a proxy of intensified silicate weathering (Palmer and Elderfield, 1985; Raymo et al., 1988; Edmond, 1992; Krishnaswami et al., 1992; Richter et al., 1992; Harris, 1995; Blum, 1997; Galy et al., 1999; Chesley et al., 2000; English et al., 2000; Bickle et al.,

HESSD
10, 8031–8069, 2013

2005). However, other studies showed that the unusual metamorphic evolution of the Himalaya had enriched carbonates to abnormally high $^{87}Sr/^{86}Sr$ ratios, and the weathering of such carbonates might control the $^{87}Sr/^{86}Sr$ ratios of river water (e.g., Edmond, 1992; Palmer and Edmond, 1992; Quade et al., 1997; Blum et al., 1998; Harris et al., 1998; English et al., 2000; Karim and Veizer, 2000; Jacobson and Blum, 2000; Bickle et al., 2001; Jacobson et al., 2002a). If much of the radiogenic Sr in river is derived from carbonate weathering then changes in seawater Sr isotopic composition would not be a proxy of the continental silicate weathering intensity.

For understanding better the contribution of silicate and carbonate weathering to Sr isotopic composition of river water, we selected two small watersheds: one was the Xishui River draining silicate rocks – a tributary of the Yangtze River, and another was the Guijiang River draining carbonate rocks – a tributary of the Pearl River. In the two river catchments, silicate and carbonate rocks accounts for about 95 % of respective drainage area. By analyzing Sr isotopic compositions of river waters, we will discuss the Sr isotope characteristics and their controlling factors in monolithologic catchment, and investigate the relationship between silicate, carbonate weathering and Sr isotope evolution of seawater.

2 Studied areas

The Xishui River is a small tributary of the Yangtze River, being located in 115°07′–116°05′ E and 30°20′–31°09′ N. It originates from the south of the Dabie Mountain (elevation 1600 m) with a length of 157 km and a drainage area of 2670 km^2. Its headwater is comprised of the Donghe River and Xihe River which converge at Yingshan County. The Xishui River merges into the Yangtze River at Lanxi (Fig. 1). The Xishui River catchment belongs to subtropical monsoon climate with a mean temperature 29 °C in summer and 4 °C in winter, and annual mean rainfall about 1350 mm. The Xishui River mainly flows across the Dabie Mountain early Proterozoic metamorphic zone which is altered by multiphase tectonism and regional metamorphism, and form a variety of metamorphic rocks and complete metamorphic facies. The catchment is covered with ultrahigh pressure metamorphic rocks mainly composed of eclogite and gneiss and some granite (Fig. 2) (Bureau of Geology and Mineral Resources of Hubei Province, 1990; China Geological Survey, 2004).

The Guijiang River, a tributary of the Pearl River, rises in the Miaoershan Mountain with an elevation of 2142 m. It has a length of 438 km and a drainage area of 18 790 km^2. The upper reaches are upwards from Rongjiang Town, and the middle reaches are from the confluence with the Lingqu River to Pingle County, which is also called "the Lijiang River", then merges into the Pearl River at Wuzhou City (Fig. 3). Annual rainfall and evaporation is about 2000 mm and 1100–1200 mm, and annual average temperature is ~ 20 °C in the Guijiang River catchment. Silurian granites, Ordovician–Cambrian shales and mud rocks intercalated carbonate rocks are mainly exposed in the headwater and upper reaches. The middle reaches are almost entirely covered with Devonian carbonate rocks, and the lower reaches flow across Cambrian terrain comprising largely carbonate rocks intercalated shales (Fig. 4) (China Geological Survey, 2004).

3 Sampling and analysis

From river mouths to source areas of the Xishui River and Guijiang River, 57 samples of river water, 1 sample of rain water, 1 sample of snow, 27 samples of riverbed sediment, and 2 samples of soil were collected during July 2010, December 2010, and July 2011, respectively (Figs. 1, 3, Table 1). Portable water quality analyzer was used to measure temperature, pH and conductivity in situ. Flow Measurement is used to measure flow velocity in field and estimate water discharge. All samples were collected from river bank or midstream away from towns to try to avoid contamination from anthropogenic activities and stored in pre-cleaned polyethylene bottles free of air. Water samples were filtered through 0.45 µm Millipore filter. An aliquot of the filtered water was acidified to pH < 2 with ultrapure grade 1 : 1 nitric acid. Sr was measured in filtered

HESSD
10, 8031–8069, 2013

and acidified water with an inductively coupled plasma spectrometer (ICP-AES, Jarrell-Ash1100) in the Center of Modern Analysis of Nanjing University. Reproducibility of measurements of Sr was checked by repeat analysis of samples and state standards in China. These repeated measurements show that in general the precision is ±5 % for Sr. Blanks were under detection limits of ICP-AES. For Sr isotope ratio analysis, Sr was separated from the samples using standard ion exchange techniques. Sr isotopic compositions were measured using a Finnigan Triton thermal ionization mass spectrometer at the State Key Laboratory for Mineral Deposits Research, Nanjing University. Reproducibility and accuracy of Sr isotope runs have been periodically checked by running the Standard Reference Material NBS 987, with a mean $^{87}Sr/^{86}Sr$ value of 0.710248 ± 20 (2σ external standard deviation, $n = 15$). The Sr isotopic ratios were normalized to $^{86}Sr/^{88}Sr = 0.1194$. The analytical blank was < 1 ng for Sr.

Only the < 63 µm fine-grained fractions of riverbed sediment and soil samples were used. The calcite in the samples was selectively dissolved with purified acetic acid solution ($0.5\,mol\,L^{-1}$) at room temperature for up to 8 h and only the silicate fractions were investigated. All of the pretreated samples were cleaned in pure water, powdered in an agate mill, and then were digested with a mixture of $HCl + HNO_3 + HClO_4 + HF$ solution. Analysis of Sr concentrations and isotopic compositions is same as water samples.

4 Results

Sr concentrations and $^{87}Sr/^{86}Sr$ ratios of water samples in the Xishui River and Guijiang River are listed in Table 2. Sr concentrations of the Xishui River are 0.468–1.70 $\mu mol\,L^{-1}$ in summer and 1.30–3.17 $\mu mol\,L^{-1}$ in winter, reflecting dilution effect from high runoff in summer. $^{87}Sr/^{86}Sr$ ratios are from 0.708686 to 0.709148 in summer and from 0.708515 to 0.709305 in winter, which do not exhibit obvious seasonal variations. Snow sample at Lanxi has Sr concentration of 0.879 mumol L^{-1} and $^{87}Sr/^{86}Sr$ ratio of 0.709495. Sr concentrations are 0.124–1.098 $\mu mol\,L^{-1}$ and $^{87}Sr/^{86}Sr$ ratios are

0.710558–0.724605 in the Guijiang River. Rainwater sample at Zhaoping has Sr concentration of 0.11 µmol L^{-1} and $^{87}Sr/^{86}Sr$ ratio of 0.710416. Comparing with the Xishui River, the Guijiang River has lower Sr concentrations but higher $^{87}Sr/^{86}Sr$ ratios. A plot of $^{87}Sr/^{86}Sr$ vs. 1/Sr shows that the typical silicate watershed Xishui River is characterized by carbonate weathering with low $^{87}Sr/^{86}Sr$ ratios and high Sr concentrations, and the typical carbonate watershed Guijiang River is closer to silicate endmember with high $^{87}Sr/^{86}Sr$ ratios and low Sr concentrations (Fig. 5). It is surprising to note that both of the two rivers exhibit entirely opposite Sr isotope characteristics to the classic silicate and carbonate weathering. The reasons will be analyzed in discussion section.

Table 2 also contains some major ion concentrations in the Xishui River (Wu et al., 2013). For the Guijiang River, we do not analyze major ion, and some data from other researchers are listed in Table 2 for references.

Sr characteristics of riverbed sediments and soils are given in Table 3. $^{87}Sr/^{86}Sr$ ratios of the Xishui riverbed sediments are 0.707058–0.712616. The Guijiang riverbed sediments have $^{87}Sr/^{86}Sr$ ratios from 0.735172 to 0.775952, and two soil samples GJ15 and GJ19 have $^{87}Sr/^{86}Sr$ ratios 0.744095 and 0.749902, respectively. $^{87}Sr/^{86}Sr$ ratios in the Guijiang River catchment are far higher than those in the Xishui River, reflecting obvious difference of Sr isotopic compositions of underlying bedrocks in the two catchments.

5 Discussions

5.1 isotope characteristics and controlling factors in the Xishui River

5.1.1 Temporal and spatial variations of Sr concentrations and isotopic compositions

Silicate rocks in the Xishui River catchment account for about 95 % of the drainage area. Among them, gneisses and are dominant, and granites are mainly distributed in the source area and Bailianhe Reservoir. Moreover, basic and ultrabasic rocks are scatteredly exposed. However, as a typical silicate watershed, the Xishui River has low $^{87}Sr/^{86}Sr$ ratios (< 0.71). The $^{87}Sr/^{86}Sr$ ratios of samples in summer decrease gradually downwards from the source area and reach the lowest value at Yinshan County (Fig. 6). After flowing across granites widely distributed around the Bailianhe Reservoir, $^{87}Sr/^{86}Sr$ ratios increase then gradually decrease from XS3 to XS1. Variation trend of $^{87}Sr/^{86}Sr$ ratios in winter is very similar to summer with an exception of XS3–XS1, which has a slightly rising trend. Variations of $^{87}Sr/^{86}Sr$ ratios may be attributed to the difference of underlying bedrocks. In the Xishui River catchment, $^{87}Sr/^{86}Sr$ ratios of Cretaceous granites are commonly higher than those of metamorphic rocks (Zheng et al., 2000; Ge et al., 2001a, b; Chen et al., 2002). Sr concentrations in the Xishui River are relatively high and the lower reaches have higher value than the headwaters. The samples XS8–XS4 in summer and winter have similar increasing trend of Sr concentrations. However, variation trend of samples XS3–XS1 between summer and winter is remarkably different, reflecting in very high Sr concentrations of samples XS3 and XS1 in winter. Moreover, concentrations of major ion Ca^{2+}, Mg^{2+}, and HCO_3^- of samples XS3 and XS1 were also rather high. The 1 : 200 000 geological map (Bureau of Geology and Mineral Resources of Hubei Province, not published) shows that Archean marbles are distributed stratifiedly in the tributary Shenjiahe River and the Xishui mainstream from Lanxi Town to Xishui County. Therefore, high concentrations of Ca^{2+}, Mg^{2+}, HCO_3^-, and Sr in the two samples may be caused by stronger carbonate weathering in the watersheds.

Seasonally, Sr concentrations in summer are obviously lower than those in winter, reflecting dilution effect resulted from increasing discharge. Variations of $^{87}Sr/^{86}Sr$ ratios are slight and do not exhibit notable regularity. In general, the Xishui River does not match the characteristics of typical silicate watershed which commonly has low Sr concentrations and high $^{87}Sr/^{86}Sr$ ratios. As the Xishui River only has a length of 157 km, climate effect (temperature, rainfall and evaporation etc.) among different samples can be negligible. In field reconnaissance we found that vegetation type and coverage was similar in the catchment. In a companion paper, silicate weathering rates are 0.64–4.44 t km^{-2} yr^{-1} in winter and 4.07–21.2 t km^{-2} yr^{-1} in summer, and carbonate weathering rates are 0.39–3.57 t km^{-2} yr^{-1} and 1.70–14.1 t km^{-2} yr^{-1} for winter and summer, respectively (Wu et al., 2013). It indicates that climate is an important controlling factor on chemical weathering. In comparison, ^{87}Sr/^{86}Sr ratios between summer and winter show small difference, which seemingly suggests the weak influence of climate. However, as silicate rocks exposed in the Xishui River catchment have similarly low ^{87}Sr/^{86}Sr ratios with carbonate rocks (Table 4), it is difficult to distinguish between the influence of climate on silicate and carbonate weathering rates and then on their Sr isotopic compositions. In Table 4, we compile some Sr isotopic data of bedrocks in the Xishui River catchment. ^{87}Sr/^{86}Sr ratios of these silicate rocks are low and relatively homogeneous with small variation range. Therefore, ^{87}Sr/^{86}Sr ratios of underlying bedrocks are certainly important controlling factor on the Sr isotope characteristics in the Xishui River, but influence of climate is uncertainty.

Moreover, different land use (agricultural, industrial, and residential use) introduces new sources of weatherable Sr into rivers. Jiang et al. (2009) and Li et al. (2010) investigated groundwater in cultivated land, grass land, construction land, and forest land, industrial and domestic waste in southwest China and gave ^{87}Sr/^{86}Sr ratios of 0.70762–0.71273. ^{87}Sr/^{86}Sr ratios of 24 fertilizers commonly used in Spain are 0.703350–0.715216 with an average of 0.70823 (Vitòria et al., 2004). Brenot et al. (2008) gave ^{87}Sr/^{86}Sr ratios of liquid and solid fertilizers (0.708078 and 0.703313, respectively) in their studies on a small catchment in the Paris basin. ^{87}Sr/^{86}Sr ratios of 12 plants are 0.70856–0.71145 in Guizhou Province (Zheng et al., 2008) (Table 5). As ^{87}Sr/^{86}Sr ratios of these potential sources are close to those in the Xishui river water, it is difficult to separate respective contribution. In next section, we will try to use inversion model to identify the influence of anthropogenic activities.

HESSD
10, 8031–8069, 2013

5.1.2 Source of Sr in the Xishui River

Sr in river water is mainly from atmospheric input (Sr_{atm}), anthropogenic activities (urban sewage (Sr_{urb}) and agricultural activities (Sr_{agr})), silicate weathering (Sr_{sil}), carbonate weathering (Sr_{carb}), and evaporite dissolution (Sr_{ev}) (Galy and France–Lanord, 1999). To quantify the relative contribution of the six endmembers, an inversion model is used (Négrel et al., 1993; Gaillardet et al., 1999; Millot et al., 2003; Wu et al., 2005; Chetelat et al., 2008). The set of mass balance equations are (Negrél et al., 1993; Gaillardet et al., 1999):

$$\left(\frac{X}{Na}\right)_{river} = \sum_i \left(\frac{X}{Na}\right)_i \alpha_{i,Na} \quad (1)$$

$$\left(\frac{^{87}Sr}{^{86}Sr}\right)_{river}\left(\frac{Sr}{Na}\right)_{river} = \sum_i \left(\frac{^{87}Sr}{^{86}Sr}\right)_i \left(\frac{Sr}{Na}\right)_i \alpha_{i,Na} \quad (2)$$

Where X represents Ca, Mg, K, Cl, NO_3, and Sr, i is six endmembers, and $\alpha_{i,Na}$ is the respective mass fractions of Na in different sources. The closure equation is:

$$\sum_i \alpha_{i,Na} = 1 \quad (3)$$

Although the Xishui River is a typical silicate watershed, lithologies in the catchment are complex and carbonate rocks are distributed stratifiedly and lenticularly in metamorphic rocks. Therefore, the Na normalized ratios analyzed in the Xishui River are not suitable for representing silicate endmember. For the Na normalized ratios of silicate endmember, the data of some “truly small watersheds draining silicate rocks” (with drainage area $< 10\,km^2$) are referred (Edmond et al., 1994; White and Blum, 1995; Oliva et al., 2003). The ratios are 0.2–1.0 for Ca/Na, 0.15–0.5 for Mg/Na, 0.1–0.3 for K/Na, 0.002–0.004 for Sr/Na, and 0 for Cl/Na and NO_3/Na (Wu et al., 2013).

HESSD
10, 8031–8069, 2013

For the other five endmembers, Na normalized ratios in the Yangtze River from other authors are used (Chetelat et al., 2008 and references therein). For every sample, we can solve for 6 model parameters using 8 mass balance equations. It belongs to overdetermined equations with infinite solutions. The Global Optimization program is processed, which computes the 'a posteriori' set of values and propagates the errors in the least-squares sense. Calculated contributions of different sources to Sr in river are listed in Table 6.

In Table 6, Sr in the Xishui River is mainly from silicate weathering, atmospheric input, and carbonate weathering, then followed by contribution of evaporite dissolution. Influence of anthropogenic activities is negligible. Though the distributed area of carbonate rocks is only < 5 % of the drainage area, it has a disproportionately important contribution to the Sr in the Xishui River (average 19 %), being consistent with the conclusion of studies on major ions (Wu et al., 2013). Previous studies indicated that trace calcite in small watersheds draining silicate rocks could contribute a large proportion to major ions in river (Blum et al., 1998; Jacobson et al., 2002b; Oliva et al., 2004). As $^{87}Sr/^{86}Sr$ ratios of silicate rocks in the Xishui River catchment are very close to those of Paleozoic carbonate rocks in the Yangtze Platform (Table 4), even if the contribution from carbonate weathering to Sr far exceeds its distributed area, it still has no obvious decreasing influence on the $^{87}Sr/^{86}Sr$ ratios of river water.

5.2 Sr isotope characteristics and controlling factors in the Guijiang River

5.2.1 Spatial variations of Sr concentrations and isotopic compositions

The Guijiang River flows across the karst region intercalated by detrital rocks, sand rocks, mud rocks and shales in southern China and granites are only exposed in the source area Miaoershan Mountain and the upper reaches of the tributary Siqin River. $^{87}Sr/^{86}Sr$ ratios are 0.719558–0.724605 and Sr concentrations are 0.124–1.098 µmol L^{-1} in the Guijiang River. There is strongly positive correlation between $^{87}Sr/^{86}Sr$ vs. 1/Sr (r^2 = 0.81), indicating two-component mixing between silicate and

HESSD
10, 8031–8069, 2013

carbonate weathering. Studies from other researchers showed that granites in the Guijiang River catchment were characterized by extremely high $^{87}Sr/^{86}Sr$ ratios with an average of about 0.8 (Table 4). Moreover, $^{87}Sr/^{86}Sr$ ratios of silicate fraction of the riverbed sediments and soils in the Guijiang River catchment are from 0.735172 to 0.775952 with an average of 0.745891, indicating that these silicate components have high Sr isotope values. $^{87}Sr/^{86}Sr$ ratios of soils in karst cave and in profiles in the neighboring Guizhou Province are 0.727317–0.727417 and 0.71049–0.72266 (Liu et al., 2011; Zhu et al., 2011). As groundwater in different land use area, industrial and domestic waste, fertilizer, and plant have low $^{87}Sr/^{86}Sr$ ratios (almost entirely < 0.71, Table 5), they are not the source of high Sr isotopic compositions of the Guijiang river water. Therefore, those silicate components contained in the karst area should be the most important endmember controlling the Sr isotopic characteristics of the river water. As we lack Sr isotope data of carbonate rocks in the Guijiang River catchment, $^{87}Sr/^{86}Sr$ ratios of the Late Paleozoic marine carbonate rocks in the Yangtze Platform and karst area of neighboring province are used as another endmember (0.705890–0.708907, Huang, 1997; Zeng et al., 2007; Liu et al., 2011. Table 4). These carbonate rocks are very close to those in the Guijiang River catchment in age, and so their $^{87}Sr/^{86}Sr$ ratios are used in many studies in karst area in Southwest China (e.g. Han et al., 2004, 2010; Jiang et al., 2011).

In the following we only discuss the spatial variations of $^{87}Sr/^{86}Sr$ ratios because of strongly positive correlation between $^{87}Sr/^{86}Sr$ vs. 1/Sr in the Guijiang River. $^{87}Sr/^{86}Sr$ ratios in the mainstream are from 0.710558 to 0.716453 and exhibit an obvious variation trend (Fig. 7). High values of the headwater samples S1 and S3 (0.715849 and 0.715973) can be attributed to granites in the Miaoershan Mountain with extremely high $^{87}Sr/^{86}Sr$ ratios (Table 4). With abundant exposure of carbonate rocks and import of fertilizer, urban runoff, and municipal water with low Sr isotope values (Tables 4, 5), $^{87}Sr/^{86}Sr$ ratios obviously decrease downwards from the source area. The sample S5 has the lowest $^{87}Sr/^{86}Sr$ ratio in the Guijiang River, because the Sr isotopic compositions of Carboniferous carbonate rocks are the lowest in late Paleozoic (Huang, 1997). $^{87}Sr/^{86}Sr$ ratios of the mainstream remarkably rise from samples S5 to S10, and gradually decrease from S12 to S15, then fluctuate from S17 to S22. The variation trend is inconsistent with the $^{87}Sr/^{86}Sr$ ratios of tributaries and so it does not result from confluence of these tributaries. Previous studies on karst water showed that the water draining sand rocks had the highest $^{87}Sr/^{86}Sr$ ratios followed by dolomites then limestones (Wang and Wang, 2005). Therefore, variation of $^{87}Sr/^{86}Sr$ ratios in these reaches may be attributed to the subtle differences of underlying bedrocks and/or anthropogenic influence. After flowing through Pingle County, $^{87}Sr/^{86}Sr$ ratios progressively increase and reach the highest value near the river mouth. The Guijiang River catchment downwards from Pingle flows across Cambrian strata comprising carbonate rocks intercalated by sand rocks, mud rocks, and shales, which have higher $^{87}Sr/^{86}Sr$ ratios than those of Devonian and Carboniferous (Burke et al., 1982; Huang, 1997). Considering low $^{87}Sr/^{86}Sr$ ratios of carbonate rocks, vegetation, fertilizer, industrial and domestic wastewater, high Sr isotopic values of the Guijiang river water should be caused by silicate weathering, which is consistent with high $^{87}Sr/^{86}Sr$ ratios of silicate fraction of riverbed sediment and soil in catchment. The tributaries Longjiang River and Siliang River have the highest $^{87}Sr/^{86}Sr$ ratios in the whole Guijiang River. As the two tributaries are small enough, silicate components exposed scatteredly can have an important influence on $^{87}Sr/^{86}Sr$ ratios of river water.

Generally, $^{87}Sr/^{86}Sr$ ratios of the Guijang River are far higher than those of the upper and middle Pearl River (the Nanpan River of 0.70740–0.70856, Xu and Liu, 2007, and the Xijiang River of 0.70837–0.71049, Wang et al., 2009), also higher than those of the tributaries Wujiang River (0.707722–0.711037) and Yuanjiang River draining karst region (0.708711–0.714479) of the Yangtze River (Han and Liu, 2004). This suggests that although the Guijiang River is typical karst river, a few silicate components such as granites, sand rocks, mud rocks, and shales with high Sr isotopic compositions have very important contribution to the $^{87}Sr/^{86}Sr$ ratios of river water.

5.2.2 Source of Sr in the Guijiang River

As we lack the data of major ions in the Guijiang River, the inversion calculation cannot be used to quantify the contribution of different reservoirs to Sr in the river. Under this circumstance, we only roughly evaluate the contributions of silicate and carbonate weathering to Sr. For this purpose, we neglect the contributions of anthropogenic activities and evaporite dissolution and simplify the reservoirs to only silicate and carbonate weathering. The simple equations are:

$$X1(^{87}Sr/^{86}Sr)_{carb} + X2(^{87}Sr/^{86}Sr)_{sil} = (^{87}Sr/^{86}Sr)_{river} \quad (4)$$

$$X1 + X2 = 1 \quad (5)$$

Where $(^{87}Sr/^{86}Sr)_{carb}$ is average $^{87}Sr/^{86}Sr$ ratio of carbonate rocks in the catchment. From the samples S1 to S25, underlying bedrocks are mainly Devonian and Carboniferous carbonate rocks with an average $^{87}Sr/^{86}Sr$ ratio of 0.708075, and the river reaches downwards from S26 flow across Cambrian strata with an average $^{87}Sr/^{86}Sr$ ratio of 0.7091 (Burke et al., 1982; Huang, 1997). $(^{87}Sr/^{86}Sr)_{sil}$ represents average $^{87}Sr/^{86}Sr$ ratio of silicate components in the catchment which is about 0.75 (Table 4). X1 and X2 is the contribution proportion of carbonate and silicate weathering. Calculated X1 is 62.1–95.8 % (average 88.6 %) and X2 is 4.2–37.9 % (average 11.4 %). Though the contribution from silicate weathering is small, it remarkably raises the $^{87}Sr/^{86}Sr$ ratios of the Guijiang River water owing to high Sr isotopic compositions.

5.3 Influence on the Sr isotope evolution of seawater and implication

The significance of river for variations in seawater $^{87}Sr/^{86}Sr$ ratios mainly depends on both the Sr fluxes and their $^{87}Sr/^{86}Sr$ ratios. This can be assessed by calculating an "excess ^{87}Sr flux" ($^{87}Sr_{ex}$) (Bickle et al., 2003):

$$^{87}Sr_{ex} = (^{87}Sr/^{86}Sr - 0.70916) \times Sr_{flux} \quad (6)$$

HESSD
10, 8031–8069, 2013
Sr isotopic characteristics in small watersheds
W. H. Wu et al.

Where Sr_{flux} is Sr fluxes transported by rivers and 0.70916 represents $^{87}Sr/^{86}Sr$ in modern seawater (Hodell et al., 1990). The $^{87}Sr_{ex}$ of the Xishui River at Lanxi is $-0.29 \times 10^3\,mol\,yr^{-1}$ and $-1.6 \times 10^3\,mol\,yr^{-1}$ in winter and summer, respectively. The negative values show that the Xishui River will cut down the Sr isotopic compositions of seawater as a typical silicate watershed. As well as for some rivers draining young basalts, they have low $^{87}Sr/^{86}Sr$ ratios and cannot result in noticeable increase of the Sr isotopic compositions of seawater. For example, Yale and Carpenter (1996) observed a correlation between the formation of large basalt provinces and decreases in the Sr isotope ratio of the ocean. Taylor and Lasaga (1999) studied the contribution of chemical weathering of the young Columbia basalts to the Sr isotope evolution of seawater. They concluded that sharp decreases in marine $^{87}Sr/^{86}Sr$ ratios reflected periods of increased global weathering rates, and young and older lithologic variations could be one of the major controlling factors on the marine Sr isotope record. Allègre et al. (2010) proposed that intensive weathering on volcanic islands, island arcs and oceanic islands was the missing source of mantle-derived $^{87}Sr/^{86}Sr$ (0.703) in seawater Sr isotope balance and represented about 60 % of the actual mantle-like input of Sr to the oceans. On the other hand, many studies in recent years showed that the global flux of CO_2 consumed by chemical weathering of basalts represented 30–35 % of the consumption flux of continental silicate (e.g. Gaillardet et al., 1999; Dessert et al., 2003; Dupré et al., 2003). In this case, river catchments with high silicate weathering rates do not transport highly radiogenic Sr into oceans. Therefore, it may be questionable that using of Sr isotope ratio variations of seawater to deduce the continental silicate weathering intensity.

According to the Eq. (6), the $^{87}Sr_{ex}$ of the Guijiang River at Wuzhou is $56.1 \times 10^3\,mol\,yr^{-1}$. As a typical carbonate watershed, the Guijiang River has a positive effect on the increase of seawater Sr isotope ratio. Though this effect is weak (only accounts for 0.1 % of $^{87}Sr_{ex}$ in the global rivers ($83 \times 10^6\,mol\,yr^{-1}$, Davis et al., 2003)) owing to small discharge, it is mainly from the weathering of silicate components exposed in the catchment. Therefore, simple discussions of either silicate or carbonate

HESSD
10, 8031–8069, 2013

weathering dominating the seawater $^{87}Sr/^{86}Sr$ ratio evolution are insufficient, and the Sr isotopic compositions of underlying bedrocks in catchment must also be considered.

6 Conclusions

As a typical small silicate watershed, the Xishui River has relatively high Sr concentrations and low $^{87}Sr/^{86}Sr$ ratios. An important reason is gneisses and granites widely distributed in the catchment has rather low Sr isotope ratios. Large difference of chemical weathering rates in summer and winter indicates significant influence of climate regime. However, its influence on Sr isotope is uncertainty owing to very similar Sr isotope values between silicate and carbonate rocks in the Xishui River catchment. The $^{87}Sr_{ex}$ of the Xishui River at Lanxi is -0.29×10^3 mol yr^{-1} and -1.6×10^3 mol yr^{-1} in winter and summer, respectively, indicating that the Xishui River decreases the Sr isotope values of seawater. Considering low $^{87}Sr/^{86}Sr$ ratios of young basalts, they may also reduce the seawater Sr isotope ratios. However, silicate weathering rates in these river catchments are very high and so affect importantly the atmospheric CO_2 consumption and the global climate change. In this sense, there is no directly corresponding relationship between silicate weathering intensity and sea water Sr isotope evolution. By contrast, the Guijiang River has low Sr concentrations and high $^{87}Sr/^{86}Sr$ ratios as a typical small carbonate watershed, being mainly attributed to the weathering of silicate components exposed in the catchment. The $^{87}Sr_{ex}$ of the Guijiang River at Wuzhou is 56.1×10^3 mol yr^{-1}, and the positive value shows that it will raise the seawater Sr isotope ratio after transporting into oceans. Therefore, discussions of either silicate or carbonate weathering dominating the seawater $^{87}Sr/^{86}Sr$ ratio evolution are problematic without connecting with studies on the Sr isotope ratios of underlying bedrocks.

HESSD
10, 8031–8069, 2013

Acknowledgements. This study was supported by China Geological Survey Projects (Grant No. Water [2010] Mineral Evaluation 03-07-08), the 863 Projects (Grant No. 2009AA06Z112), and the Natural Science Foundation of China (Project No. 40830107, 40873001 and 41003001). We thank Zhou Bin, Luo Chao, Zhang Qiang, Zhang Chunlai et al. for their helps in the field and Pu Wei in the laboratory works.

References

Allègre, C. J., Louvat, P., Gaillardet, J., Meynadier, L., Rad, S., and Capmas, F.: The fundamental role of island arc weathering in the oceanic Sr isotope budget, Earth Planet. Sci. Lett., 292, 51–56, 2010.

Bickle, M. J., Bunbury, J., Chapman, H. J., Harris, N. B. W., Fairchild, I. J., and Ahmad, T.: Fluxes of Sr into the headwaters of the Ganges, Geochim. Cosmochim. Acta, 67, 2567–2584, 2003.

Bickle, M. J., Chapman, H. J., Bunbury, J., Harris, N. B. W., Fairchild, I. J., Ahmad, T., and Pomiès, C.: Relative contributions of silicate and carbonate rocks to riverine Sr fluxes in the headwaters of the Ganges, Geochim. Cosmochim. Acta, 69, 2221–2240, 2005.

Bickle, M. J., Harris, N. B. W., Bunbury, J. Chapman, H. J., Fairchild, I. J., and Ahmad, T.: Controls on the $^{87}Sr/^{86}Sr$ of carbonates in the Garwal Himalaya, headwaters of the Ganges, J. Geol., 109, 737–753, 2001.

Blum, J. D.: The effect of late Cenozoic glaciation and tectonic uplift on silicate weathering rates and the marine $^{87}Sr/^{86}Sr$ record, in: Tectonic Uplift and Climate Change, edited by: Ruddiman, W. R., Plenum, New York, 260–288, 2007.

Blum, J. D., Gazis, C. A., Jacobson, A. D., and Chamberlain, C. P.: Carbonate versus silicate weathering in the Raikhot watershed within the High Himalayan Crystalline Series, Geology, 26, 411–414, 1998.

Brass, G. W.: The variation of the marine $^{87}Sr/^{86}Sr$ ratio during Phanerozoic time: Interpretation using a flux model, Geochim. Cosmochim. Acta, 40, 721–730, 1976.

Brenot, A., Baran, N., Petelet-Giraud, E., and Négrel, P.: Interaction between different water bodies in a small catchment in the Paris basin (Brévilles, France), Tracing of multiple Sr sources through Sr isotopes coupled with Mg/Sr and Ca/Sr ratios, Appl. Geochem., 23, 58–75, 2008.

Bureau of Geology and Mineral Resources of Hubei Province: Regional Geology of Hubei Province, Beijing, Geological Publishing House, 1990 (in Chinese).
Burke, W. H., Denison, R. E., Hetherington, E. A., Koepnick, R. B., Nelson, H. F., and Otto, J. B.: Variation of seawater $^{87}Sr/^{86}Sr$ throughout Phanerozoic time, Geology, 10, 516–519, 1982.
Capo, R. C. and DePaolo, D. J.: Seawater strontium isotopic variations from 2.5 million years ago to the present, Science, 249, 51–55, 1990.
Chen, B., Jahn, B. M., and Wei, C. J.: Petrogenesis of Mesozoic granitoids in the Dabie UHP complex, Central China: trace element and Nd–Sr isotope evidence, Lithos, 60, 67–88, 2002.
Chesley, J. T., Quade, J., and Ruiz, J.: The Os and Sr isotopic record of Himalayan paleorivers: Himalayan tectonics and influence on ocean chemistry, Earth Planet. Sci. Lett., 179, 115–124, 2000.
Chetelat, B., Liu, C. Q., Zhao, Z. Q., Wang, Q. L., Li, S. L., and Wang, B. L.: Geochemistry of the dissolved load of the Changjiang Basin rivers: Anthropogenic impacts and chemical weathering, Geochim. Cosmochim. Acta, 72, 4254–4277, 2008.
China Geological Survey: Geological Map of the People's Republic of China 1:2 500 000, SinoMaps Press, Beijing, 2004.
Davis, A. C., Bickle, M. J., and Teagle, D. A. H.: Imbalance in the oceanic strontium budget, Earth Planet. Sci. Lett., 211, 173–187, 2003.
DePaolo, D. J.: Detailed record of the Neogene Sr isotopic evolution of seawater from DSDP Site 590B, Geology, 14, 103–106, 1986.
DePaolo, D. J. and Ingram, B. L.: High-Resolution Stratigraphy with Strontium Isotopes, Science, 227, 938–941, 1985.
Derry, L. A. and France-Lanord, C.: Neogene Himalayan weathering history and river $^{87}Sr/^{86}Sr$: impact on the marine Sr record, Earth Planet. Sci. Lett., 142, 59–74, 1996.
Dessert, C., Dupré, B., Gaillardet, J., François, L. M., and Allègre, C. J.: Basalt weathering laws and the impact of basalt weathering on the global carbon cycle, Chem. Geol., 202, 257–273, 2003.
Dupré, B., Dessert, C., Oliva, P., Goddéris, Y., Viers, J., François, L., Millot, R., and Gaillardet, J.: Rivers, chemical weathering and Earth's climate, C. R. Geosci., 335, 1141–1160, 2003.
Edmond, J. M.: Himalayan tectonics, weathering processes, and the strontium isotope record in marine limestones, Science, 258, 1594–1597, 1992.

Edmond, J. M., Palmer, M. R., Measures, C. I., Grant, B., and Stallard, R. F.: Fluvial geochemistry and denudation rate of Guyana Shield, Geochim. Cosmochim. Acta, 59, 3301–3325, 1994.
English, N. B., Quade, J., DeCelles, P. G., and Garzione, C. N.: Geologic control of Sr and major element chemistry in Himalayan rivers, Nepal, Geochim. Cosmochim. Acta, 64, 2549–2566, 2000.
Gaillardet, J., Dupré, B., Louvat, P., and Allègre, C. J.: Global silicate weathering and CO_2 consumption rates deduced from the chemistry of large rivers, Chem. Geol., 159, 3–30, 1999.
Galy, A. and France–Lanord, C.: Weathering processes in the Ganges–Brahmaputra basin and the riverine alkalinity budget, Chem. Geol., 159, 31–60, 1999.
Galy, A., France–Lanord, C., and Derry, L. A.: The strontium isotopic budget of Himalayan rivers in Nepal and Bangladesh, Geochim. Cosmochim. Acta, 63, 1905–1925, 1999.
Ge, N. J., Li, H. Y., Hou, Z. H., Bo, L., and Qin, L. P.: Nd-Sr isotope geochemistry of the Baimajian granite in the Dabie Orogen, Geologic. Rev., 47, 184–187, 2001a (in Chinese with an English abstract).
Ge, N. J., Li, H. Y., Qin, L. P., Hou, Z. H., and Bo, L.: Sr, Nd and Pb isotope geochemistry of granulites and TTG gneisses from the North Dabie Mountains, Acta Geologi. Sinica, 75, 379–384, 2001b (in Chinese with an English abstract).
Gu, S. Y., Hua, R. M., and Qi, H. W.: Study on zircon LA-ICP-MS U-Pb dating and Sr-Nd isotope of the Guposhan granite in Guangxi, Acta Geologica Sinica, 80, 543–553, 2006 (in Chinese with an English abstract).
Han, G. L. and Liu, C. Q.: Water geochemistry controlled by carbonate dissolution: a study of the river waters draining karst–dominated terrain, Guizhou Province, China, Chem. Geol., 204, 1–21, 2004.
Han, G. L., Tang, Y., and Xu, Z. F.: Fluvial geochemistry of rivers draining karst terrain in Southwest China, J. Asian Earth Sci., 38, 65–75, 2010.
Harris, N. B. W.: Significance of weathering Himalayan metasedimentary rocks and leucogranites for the Sr-isotope evolution of seawater, Geology, 23, 795–798, 1995.
Harris, N., Bickle, M., Chapman, H., Fairchild, I., and Bunbury, J.: The significance of Himalayan rivers for silicate weathering rates: Evidence from the Bhote Kosi tributary, Chem. Geol., 144, 205–220, 1998.

HESSD
10, 8031–8069, 2013
Sr isotopic characteristics in small watersheds
W. H. Wu et al.

Hess, J., Bender, M. L., and Schilling, J. G.: Evolution of the ratio of strontium-87 to strontium-86 in seawater from Cretaceous to present, Science, 231, 979–984, 1986.
Hodell, D. A., Mead, G. A., and Mueller, P. A.: Variation in the strontium isotopic composition of seawater (8 Ma to present) implications for chemical weathering rates and dissolved fluxes to the oceans, Chem. Geol., 80, 291–307, 1990.
Hodell, D. A., Mueller, P. A., and Garrido, J. R.: Variations in the strontium isotopic composition of seawater during the Neogene, Geology, 19, 24–27, 1991.
Hosono, T., Nakano, T., Igeta, A., Tayasu, I., Tanaka, T., and Yachi, S.: Impact of fertilizer on a small watershed of Lake Biwa, Use of sulfur and strontium isotopes in environmental diagnosis, Sci. Total Environ., 384, 342–354, 2007.
Huang, S. J.: A study on carbon and strontium isotopes of late Paleozoic carbonate rocks in the upper Yangtze platform, Acta Geologica Sinica, 71, 45–53, 1997 (in Chinese with an English abstract).
Jacobsen, A. D. and Blum, J. D.: Ca/Sr and $^{87}Sr/^{86}Sr$ geochemistry of disseminated calcite in Himalayan silicate rocks from Nanga Parbat: Influence on river-water chemistry, Geology, 28, 463–466, 2000.
Jacobson, A. D., Blum, J. D., Chamberlain, C. P., Poage, M. A., and Sloan, V.F.: Ca/Sr and Sr isotope systematics of a Himalayan glacial chronosequence: Carbonate versus silicate weathering rates as a function of landscape surface age, Geochim. Cosmochim. Acta, 66, 13–27, 2002a.
Jacobsen, A. D., Blum, J. D., and Walter, L. M.: Reconciling the elemental and Sr isotope composition of Himalayan weathering fluxes: Insights from the carbonate geochemistry of stream waters, Geochim. Cosmochim. Acta, 66, 3417–3429, 2002b.
Jahn, B. M., Wu, F. Y., Lo, C. H., and Tsai, C. H.: Crust-mantle interaction induced by deep subduction of the continental crust: geochemical and Sr-Nd isotopic evidence from post-collisional mafic-ultramafic intrusions of the northern Dabie complex, central China, Chem. Geol., 157, 119–146, 1999.
Jiang, Y. J., Wu, Y. X., and Yuan, D. X.: Human impacts on karst groundwater contamination deduced by coupled nitrogen with strontium isotopes in the Nandong underground river system in Yunan, China, Environ. Sci. Technol., 43, 7676–7683, 2009.
Karim, A. and Veizer, J.: Weathering processes in the Indus River Basin: implications from riverine carbon, sulfur, oxygen, and strontium isotopes, Chem. Geol., 170, 153–177, 2000.

HESSD
10, 8031–8069, 2013

Korte, C., Jasper, T., Kozur, H. W., and Veizer, J.: $^{87}Sr/^{86}Sr$ record of Permian seawater, Palaeogeogr. Palaeocl., 240, 89–107, 2006.
Krishnaswami, S., Trivedi, J. R., Sarin, M. M., Ramesh, R., and Sharma, K. K.: Strontium isotopes and Rubidium in the Ganga-Brahmaputra river system: Weathering in the Himalaya, fluxes to the Bay of Bengal and contributions to the evolution of oceanic $^{87}Sr/^{86}Sr$, Earth Planet. Sci. Lett., 109, 243–253, 1992.
Lang, Y. C., Liu, C. Q., Zhao, Z. Q., Li, S. L., and Han, G. L.: Geochemistry of surface and ground water in Guiyang, China: Water/rock interaction and pollution in a karst hydrological system, Appl. Geochem., 21, 887–903, 2006.
Li, S. G., Nie, Y. H., Hart, S. R., and Zhang, Z. Q.: Interaction between subducted continental crust and the mantle – II. Sr and Nd isotopic geochemistry of the syncollisional mafic-ultramafic intrusions in Dabie Mountains, Sci. China Ser. D, 41, 632–638, 1998.
Li, X. D., Liu, C. Q., Harue, M., Li, S. L., and Liu, X. L.: The use of environmental isotopic (C, Sr, S) and hydrochemical tracers to characterize anthropogenic effects on karst groundwater quality: A case study of the Shuicheng Basin, SW China, Appl. Geochem., 25, 1924–1936, 2010.
Liu, W. J., Liu, C. Q., Zhao, Z. Q., Li, L. B., Tu, C. L., and Liu, T. Z.: The weathering and soil formation process in karstic area, southwest China: A study on strontium isotope geochemistry of yellow and limestone soil profiles, J. Earth Environ., 2, 331–336, 2011 (in Chinese with an English abstract).
Liu, Y. C., Xu, S. T., Li, S. G., Jiang, L. L., Wu, W. P., Chen, G. B., and Su, W.: Geochemical characteristics, Sr-Nd isotopic compositions and tectonic implications of eclogite in the North Dabie, Sci. China Ser. D, 30, 99–107, 2000 (in Chinese).
Melezhik, V. A., Pokrovsky, B. G., Fallick, A. E., Kuznetsov, A. B., and Bujakaite, M. I.: Constraints on $^{87}Sr/^{86}Sr$ of late Ediacaran seawater: insight from Siberian high-Sr limestones, J. Geol. Soc. London, 166, 183–191, 2009.
Millot, R., Gaillardet, J., Dupré, B., and Allègre, C. J.: Northern latitude chemical weathering rates: Clues from the Mackenzie River Basin, Canada, Geochi. Cosmochi. Acta, 67, 1305–1329, 2003.
Négrel, P., Allègre, C. J., Dupré, B., and Lewin, E.: Erosion sources determined by inversion of major and trace element ratios and strontium isotopic ratios in river water; the Congo Basin case, Earth Planet. Sci. Lett., 120, 59–76, 1993.

HESSD
10, 8031–8069, 2013
Sr isotopic characteristics in small watersheds
W. H. Wu et al.

Palmer, M. R. and Edmond, J. M.: The strontium isotope budget of the modern ocean, Earth Planet. Sci. Lett., 92, 11–26, 1989.
Palmer, M. R. and Edmond, J. M.: Controls over the strontium isotope composition of river water, Geochim. Cosmochim. Acta, 56, 2099–2111, 1992.
Palmer, M. R. and Elderfield, H.: Sr isotope composition of seawater over the past 75 Myr, Nature, 314, 526–528, 1985.
Oliva, P., Viers, J., and Dupré, B.: Chemical weathering in granitic environments, Chem. Geol., 202, 225–256, 2003.
Oliva, P., Dupré, B., Martin, F., and Viers, J.: The role of trace minerals in chemical weathering in a high-elevation granitic watershed (Estibere, France): Chemical and mineralogical evidence, Geochim. Cosmochim. Acta, 68, 2223–2244, 2004.
Quade, J., Roe, L., DeCelles, P. G., and Ojha, T. P.: The late Neogene $^{87}Sr/^{86}Sr$ record of lowland Himalayan rivers, Science, 276, 1828–1831, 1997.
Raymo, M. E., Ruddiman, W. F., and Froelich, P. N.: Influence of Late Cenozoic mountain building on ocean geochemical cycles, Geology, 16, 649–653, 1988.
Richter, F. M. and DePaolo, D. J.: Numerical models for diagenesis and the Neogene Sr isotopic evolution of seawater from DSDP Site 590B, Earth Planet. Sci. Lett., 83, 27–38, 1987.
Richter, F. M. and DePaolo, D. J.: Diagenesis and Sr isotopic evolution of seawater using data from DSDP 590B and 575, Earth Planet. Sci. Lett., 90, 382–394, 1988.
Richter, F. M., Rowley, D. B., and DePaolo, D. J.: Sr isotope evolution of seawater: the role of tectonics, Earth Planet. Sci. Lett., 109, 11–23, 1992.
Singh, S. K., Kumar, A., and France-Lanord, C.: Sr and $^{87}Sr/^{86}Sr$ in waters and sediments of the Brahmaputra river system: Silicate weathering, CO_2 consumption and Sr flux, Chem. Geol., 234, 308–320, 2006.
Taylor, A. S. and Lasaga, A. C.: The role of basalt weathering in the Sr isotope budget of the oceans, Chem. Geol., 161, 199–214, 1999.
Veizer, J.: Strontium isotopes in seawater through time, Ann. Rev. Planet. Sci., 17, 141–167, 1989.
Veizer, J. and Compston, W.: $^{87}Sr/^{86}Sr$ composition of seawater during the Phanerozoic, Geochim. Cosmochim. Acta, 38, 1461–1484, 1974.
Veizer, J., Ala, D., Azmy, K., Bruckschen, P., Buhl, D., Bruhn, F., Carden, G. A. F., Diener, A., Ebneth, S., Godderis, Y., Jasper, T., Korte, C., Pawellek, F., Podlaha, O. G., and Strauss,

H.: $^{87}Sr/^{86}Sr$, $\delta^{13}C$ and $\delta^{18}O$ evolution of Phanerozoic seawater, Chem. Geol., 161, 59–88, 1999.
Vitòria, L., Otero, N., Soler, A., and Canals, A.: Fertilizer characterization: isotopic data (N, S, O, C, and Sr), Environ. Sci. Technol., 38, 3254–3262, 2004.
Wang, B., Lee, X. Q., Yuan, H. L., Zhou, H., and Zhao, Y. L.: Geochemical characteristics of main ion and Sr isotope in the main channel of Xijiang River, South China, Geochimica, 38, 345–353, 2009 (in Chinese with an English abstract).
Wang, T. and Wang, Z. Y.: $^{87}Sr/^{86}Sr$ characteristics of karst water in Guilin area, Acta Geoscientica Sinica, 26 supplement, 299–302, 2005 (in Chinese with an English abstract).
Wang, Y. J., Fan, W. M., Peng, T. P., Zhang, H. F., and Guo, F.: Nature of the Mesozoic lithospheric mantle and tectonic decoupling beneath the Dabie Orogen, Central China: Evidence from $^{40}Ar/^{39}Ar$ geochronology, elemental and Sr-Nd-Pb isotopic compositions of early Cretaceous mafic igneous rocks, Chem. Geol., 220, 165–189, 2005.
Wawrzenitz, N., Romer, R. L., Oberhänsli, R., and Dong, S. W.: Dating of subduction and differential exhumation of UHP rocks from the Central Dabie Complex (E-China): Constraints from microfabrics, Rb-Sr and U-Pb isotope systems, Lithos, 89, 174–201, 2006.
White, A. F. and Blum, A.E.: Effects of climate on chemical weathering in watersheds, Geochim. Cosmochim. Acta, 59, 1729–1747, 1995.
Wu, L. L., Huh, Y., Qin, J. H., Du, G., and Van Der Lee, S.: Chemical weathering in the Upper Huang He (Yellow River) draining the eastern Qinghai-Tibet Plateau, Geochim. Cosmochim. Acta, 69, 5279–5294, 2005.
Wu, W. H., Zheng, H. B., Yang, J. D., Luo, C., and Zhou, B.: Chemical weathering, atmospheric CO_2 consumption, and the controlling factors of small silicate watershed in subtropical zone: implications for the global carbon cycle research, Chem. Geol., revised, 2013.
Xu, W. C. and Zhang, Y. H.: Study on strontium, oxygen, neodymium and lead isotopes of Mt. Miaoershan granite batholith in south China, Guangxi Geol., 6, 15–22, 1993 (in Chinese with an English abstract).
Xu, W. C., Zhang, Y. H., and Liu, Y. B.: Progression in geochronological study and scheme of chronoclassfication on Miaoershan granite batholith, Acta Petrologica Sinica, 10, 330–337, 1994 (in Chinese with an English abstract).
Xu, Z. F. and Liu, C. Q.: Chemical weathering in the upper reaches of Xijiang River draining the Yunnan-Guizhou Plateau, Southwest China, Chem. Geol., 239, 83–95, 2007.

HESSD
10, 8031–8069, 2013
Sr isotopic characteristics in small watersheds
W. H. Wu et al.

Yale, L. B. and Carpenter, S. J.: Modeling the effects of large igneous provinces on the $^{87}Sr/^{86}Sr$ ratio of seawater, GSA Abst. Prog. A, 428, 1996.
Zeng, Y. J., Huang, S. J., Yi, T. F., Hao, X. F., Xiong, C. L., and Hu, Z. W.: Sr isotopic characteristics of carbonate rocks in Xinduqiao formation of Xikang group, western Sichuan, China, J. Earth Sci. Environment., 29, 126–129, 2007 (in Chinese with an English abstract).
Zhang, F. F., Wang, Y. J., Zhang, A. M., Fan, W. M., Zhang, Y. Z., and Zi, J. W.: Geochronological and geochemical constraints on the petrogenesis of middle Paleozoic (Kwangsian) massive granites in the eastern south China block, Lithos, 150, 188–208, 2012a.
Zhang, H. B., He, S. Y., Yu, S., Wang, Y. X., and Wang, L. L.: Hydrochemical characteristics and influencing factors of the river water in the Guijiang, Carsologica Sinica, 31, 395–401, 2012b (in Chinese with an English abstract).
Zhang, H. F., Gao, S., Zhong, Z. Q., Zhang, B. R., Zhang, L., and Hu, S. H.: Geochemical and Sr-Nd-Pb isotopic compositions of Cretaceous granitoids: constraints on tectonic framework and crustal structure of the Dabieshan ultrahigh-pressure metamorphic belt, China, Chem. Geol., 186, 281–299, 2002.
Zheng, H. Y., Liu, C. Q., Wang, Z. L., Yang, C., Chen, S., and Zhu, S. F.: Strontium isotopes as a tracer of plant nutrition element source in yellow soil region of Guizhou Province, J. Beijing Forestry Univ., 30, 72–76, 2008 (in Chinese with an English abstract).
Zheng, X. S., Jin, C. W., Zhai, M. G., and Shi, Y. H.: Approach to the source of the gray gneisses in North Dabie terrain: Sm-Nd isochron age and isotope composition, Acta Petrologica Sinica, 16, 194–198, 2000 (in Chinese with an English abstract).
Zhu, J. C., Li, X. D., Shen, W. Z., Wang, Y. X., and Yang, J. D.: Sr, Nd and O isotope studies on the genesis of the Huashan granite complex, Acta Geologica Sinica, 3, 225–235, 1989 (in Chinese with an English abstract).
Zhu, X. L., Wang, S. J., and Luo, W. J.: Characteristics of strontium isotopes and their implications in the Qixing Cave of Guizhou, China, Chinese Sci. Bull., 56, 670–675, 2011.

HESSD
10, 8031–8069, 2013

Table 1. The sampling information of the Xishui River and Guijiang River.

Num.	River Basins	Locations	Date	Longitude	Latitude	Ele. m	Temp. °C	pH	EC µs cm^{-1}
The Xishui River									
Winter									
XS–01[a]	Xishui R.	Lanxi	25 December 2010	115°08′40″	30°21′25″	15	9	7.7	183
XS–02[a]	Xishui R.	Guankou	25 December 2010	115°20′13″	30°32′24″	43	10.3	7.9	125
XS–03[a]	Shenjia R.	Bailianhe	25 December 2010	115°25′29″	30°37′11″	60	9.1	8	183
XS–04[a]	Xishui R.	Bailianhe	25 December 2010	115°26′20″	30°35′42″	61	10.7	7.8	122
XS–05[a]	Xihe R.	Yinshan	25 December 2010	115°38′31″	30°43′38″	101	8.2	7.9	109
XS–06[a]	Donghe R.	Yangliuwang	26 December 2010	115°44′52″	30°47′13″	131	9.2	7.8	155
XS–07[a]	Xihe R.	Jinjiapu	26 December 2010	115°37′53″	30°52′05″	126	6.2	7.86	93.1
XS–08[a]	Xihe R.	Shitouzui	26 December 2010	115°47′10″	31°01′05″	198	4.5	7.8	99.1
XS–09[a]	Xihe R.	Wujiashan	26 December 2010	115°49′35″	31°04′28″	277			
	Snow	Lanxi	25 December 2010	115°08′40″	31°04′28″	22			
Summer									
XS–01	Xishui R.	Lanxi	9 July 2011	115°08′40″	30°21′25″	15	28		126
XS–02	Xishui R.	Guankou	9 July 2011	115°20′13″	30°32′24″	43	23		142
XS–03	Shenjia R.	Bailianhe	9 July 2011	115°25′29″	30°37′11″	60	21		131
XS–04	Xishui R.	Bailianhe	9 July 2011	115°26′20″	30°35′42″	61	22		140
XS–05	Xihe R.	Yinshan	9 July 2011	115°38′31″	30°43′38″	101	28		140
XS–06	Donghe R.	Yangliuwang	9 July 2011	115°44′52″	30°47′13″	131	24		160
XS–07	Xihe R.	Jinjiapu	9 July 2011	115°37′53″	30°52′05″	126	22		133
XS–08	Xihe R.	Shitouzui	9 July 2011	115°47′10″	31°01′05″	198	20		109
The Guijiang River									
GJ–01[a]	Lin R.	Rongjiang	26 July 2010	110°28′36″	25°33′48″	184	28	7.99	236
GJ–02[a]	Darong R.	Rongjiang	26 July 2010	110°28′18″	25°33′52″	186	27.6	7.37	71
GJ–03[a]	Li R.	Rongjiang	26 July 2010	110°27′26″	25°33′14″	179	27.3	7.39	74
GJ–04	Gantang R.	Tanxia	27 July 2010	110°17′28″	25°27′25″	168	25	7.58	152
GJ–05	Li R.	Guilin	27 July 2010	110°19′38″	25°21′19″	154	28.2	7.62	170
GJ–06	Taohua R.	Guilin	27 July 2010	110°17′02″	25°16′32″	153	28.5	7.27	229
GJ–07	Li R.	Guilin	27 July 2010	110°18′58″	25°13′53″	148	28.1	7.3	172
GJ–08	Li R.	Zhemu	27 July 2010	110°20′58″	25°12′13″	146	28.7	7.31	166
GJ–09[a]	Liangfeng R.	Zhemu	27 July 2010	110°21′04″	25°11′59″	147	29.8	7.41	316
GJ–10[a]	Li R.	Majiafang	27 July 2010	110°23′13″	25°10′44″	141	29.3	7.41	177
GJ–11[a]	Chaotian R.	Daxu	27 July 2010	110°25′45″	25°10′38″	136	30.6	8.56	207
GJ–12	Li R.	Guanyan	27 July 2010	110°26′52″	25°03′16″	128	30.5	8.38	182
GJ–13	Underground R.	Guanyan	27 July 2010	110°27′25″	25°02′57″	129	22.3	8.13	258
GJ–14	Li R.	Guanyan	27 July 2010	110°27′14″	25°02′38″	128	30.5	8.31	182
GJ–15[b]	Li R.	Xinping	27 July 2010	110°31′07″	24°55′20″	118	29.8	7.73	185
GJ–16	Longjin R.	Xinping	28 July 2010	110°31′35″	24°55′04″	119	28.6	7.77	228
GJ–17	Li R.	Xinping	28 July 2010	110°31′05″	24°54′45″	118	29.8	7.78	186

Table 1. Continued.

Num.	River Basins	Locations	Date	Longitude	Latitude	Ele.	Temp.	pH	EC
						m	°C		$\mu s\,cm^{-1}$
GJ–18	Li R.	Yangshuo	28 July 2010	110°30′00″	24°46′10″	112	30.5	8.14	189
GJ–19[b]	Yulong R.	Yangshuo	28 July 2010	110°30′40″	24°46′05″	112	31.2	8.1	238
GJ–20[a]	Li R.	Yangshuo	28 July 2010	110°31′02″	24°46′42″	112	30.6	8.2	193
GJ–21	Li R.	Pingle	28 July 2010	110°36′44″	24°38′28″	104	30.5	7.98	191
GJ–22[a]	Lipu R.	Pingle	28 July 2010	110°36′43″	24°37′57″	103	30.2	7.72	159
GJ–23[a]	Li R.	Pingle	28 July 2010	110°37′40″	24°37′48″	103.5	30.3	7.96	175
GJ–24[a]	Gongcheng R.	Pingle	28 July 2010	110°38′15″	24°37′58″	104	30.4	8.01	201
GJ–25[a]	Gui R.	Pingle	28 July 2010	110°40′10″	24°37′00″	102	30.1	7.93	192
GJ–26	Gui R.	Guihua	29 July 2010	110°46′06″	24°15′31″	76	30.4	7.71	190
GJ–27	Guihua R.	Guihua	29 July 2010	110°45′46″	24°15′06″	76	30.7	8.12	164
GJ–28	Gui R.	Guihua	29 July 2010	110°47′44″	24°14′46″	75	30.3	7.78	184
GJ–29	Gui R.	Zhaoping	29 July 2010	110°50′20″	24°11′47″	55	30.3	7.81	176
GJ–30[a]	Siqin R.	Zhaoping	29 July 2010	110°50′34″	24°11′30″	55	30	8.01	142
GJ–31[a]	Gui R.	Zhaoping	29 July 2010	110°49′57″	24°10′48″	53	28	7.76	178
GJ–32	Gui R.	Majiang	29 July 2010	111°02′12″	23°53′44″	33	30.3	7.73	152
GJ–33[a]	Fuqin R.	Majiang	30 July 2010	111°02′16″	23°52′38″	34	29.4	7.64	132
GJ–34[a]	Gui R.	Majiang	30 July 2010	111°01′29″	23°52′07″	32.5	30.4	7.8	152
GJ–35	Gui R.	Changfa	30 July 2010	111°05′58″	23°43′01″	23.5	30.3	7.76	145
GJ–36	Longjiang R.	Changfa	30 July 2010	111°06′09″	23°41′51″	23	26.9	7.11	36
GJ–37	Gui R.	Changfa	30 July 2010	110°07′47″	23°38′35″	21	30.1	7.8	143
GJ–38	Gui R.	Hekou	30 July 2010	111°18′17″	23°32′29″	11	29.8	7.69	138
GJ–39	Siliang R.	Hekou	31 July 2010	111°18′32″	23°32′04″	11	28.5	6.78	89
GJ–40[a]	Gui R.	Hekou	31 July 2010	111°18′37″	23°31′30″	10	30.5	7.67	138
	Rain	Zhaoping	29 July 2010	110°49′57″	24°10′48″	53			

[a] Riverbed sediments were also collected. [b] Riverbed sediments and soils were also collected.

HESSD
10, 8031–8069, 2013

Sr isotopic characteristics in small watersheds

W. H. Wu et al.

Discussion Paper | Discussion Paper | Discussion Paper | Discussion Paper |
Title Page
Abstract Introduction
Conclusions References
Tables Figures
◀ ▶
Back Close
Full Screen / Esc
Printer-friendly Version
Interactive Discussion

Table 2. The Sr isotopic compositions and parts of major ion concentrations in the Xishui River and Guijiang River.

Num.	River Basins	Ca	Mg	K	Na	Cl	HCO_3	SO_4	NO_3	Si	Sr	$^{87}Sr/^{86}Sr$	2σ
		µmol L^{-1}											
The Xishui River[a]													
Winter													
XS-01	Xishui R.	427	201	79.2	384	149	1320	119	112	220	2.59	0.708900	3
XS-02	Xishui R.	274	125	41.1	261	92.8	872	100	46.3	197	2.10	0.708850	4
XS-03	Shengjiahe R.	491	233	49.0	361	113	1537	122	28.9	278	3.17	0.708773	6
XS-04	Xishui R.	289	131	44.8	285	86.9	918	95.4	47.3	220	2.23	0.708873	3
XS-05	Xihe R.	252	120	35.1	268	87.9	684	119	35.7	206	2.02	0.708515	4
XS-06	Donghe R.	345	153	39.4	425	126	930	155	34.2	307	2.32	0.708718	5
XS-07	Xihe R.	211	93.4	29.8	230	50.2	621	114	51.1	164	1.62	0.709305	3
XS-08	Xihe R.	231	109	28.5	218	57.0	690	118	39.8	199	1.73	0.709302	2
XS-09	Xihe R.	130	54.0	18.6	149	31.8	394	70.9	16.7	224	1.30	0.709104	2
	Snow	66.4	13.1	21.1	38.4	38.9	105	32.4	93.3	4.04	0.308	0.709495	4
Summer													
XS-01	Xishui R.	268	151	46.2	291	168	730	133	66.8	130	1.52	0.708778	3
XS-02	Xishui R.	324	151	47.0	366	155	905	127	51.6	200	1.70	0.708790	5
XS-03	Shengjiahe R.	287	138	45.4	324	140	801	116	51.1	132	1.51	0.708969	7
XS-04	Xishui R.	341	146	50.4	351	135	883	124	53.7	179	1.14	0.708999	3
XS-05	Xihe R.	313	139	43.5	361	153	847	162	55.6	194	0.468	0.708686	5
XS-06	Donghe R.	371	150	44.6	432	170	1011	146	51.6	281	0.890	0.708739	4
XS-07	Xihe R.	258	128	37.7	396	130	765	153	38.7	154	1.48	0.709043	5
XS-08	Xihe R.	250	120	33.5	263	109	603	150	32.3	153	1.39	0.709148	8
The Guijiang River[b]													
GJ–01	Lin R.										0.851	0.711293	6
GJ–02	Darong R.	286	62.6	20	60.9	48.8	370	88.5	131		0.371	0.715849	6
GJ–03	Li R.										0.389	0.715973	3
GJ–04	Gantang R.	335	21.0	8.97	21.7	27.9	630	47.3	43.4		0.576	0.712037	4
GJ–05	Li R.	797	73.3	31.8	141	134	1600	117	129		1.098	0.710558	5
GJ–06	Taohua R.										0.743	0.712451	5
GJ–07	Li R.										0.786	0.711876	6
GJ–08	Li R.										0.737	0.712369	12
GJ–09	Liangfeng R.										0.899	0.711612	4
GJ–10	Li R.										0.741	0.712728	50
GJ–11	Chaotian R.	967	128	17.7	34.4	58.4	2099	79.8	93.1		0.811	0.713659	3
GJ–12	Li R.										0.754	0.712393	35
GJ–13	Underground R.										0.743	0.712359	4
GJ–14	Li R.										0.749	0.712077	3
GJ–15	Li R.										0.745	0.712084	4
GJ–16	Longjin R.										0.764	0.714377	3

HESSD

10, 8031–8069, 2013

Table 2. Continued.

Num.	River Basins	Ca	Mg	K	Na	Cl	HCO_3	SO_4	NO_3	Si	Sr	$^{87}Sr/^{86}Sr$	2σ
		$\mu mol\,L^{-1}$											
GJ–17	Li R.										0.738	0.712204	4
GJ–18	Li R.										0.750	0.712039	4
GJ–19	Yulong R.	1327	346	20.3	57.8	97.6	3130	135	133		0.694	0.712706	5
GJ–20	Li R.	893	95.9	31.3	111	107	1754	130	73.7		0.743	0.712200	8
GJ–21	Li R.										0.746	0.712078	7
GJ–22	Lipu R.	700	189	50.8	127	121	1250	249	67.1		0.829	0.711712	6
GJ–23	Li R.										0.792	0.711911	4
GJ–24	Gongcheng R.	705	174	25.9	53.5	63.8	1320	96.1	107		0.702	0.712568	6
GJ–25	Gui R.										0.727	0.712372	3
GJ–26	Gui R.										0.711	0.712402	4
GJ–27	Guihua R.										0.615	0.712943	6
GJ–28	Gui R.										0.689	0.712483	3
GJ–29	Gui R.										0.647	0.712709	6
GJ–30	Siqin R.	743	163	46.7	118	114	1688	114	62.4		0.607	0.713242	3
GJ–31	Gui R.	816	134	35.1	99.1	98.4	1655	137	58.7		0.646	0.712750	7
GJ–32	Gui R.										0.567	0.713365	4
GJ–33	Fuqin R.	478	145	45.6	82.2	88.6	1100	90.6	60.2		0.697	0.712798	4
GJ–34	Gui R.										0.576	0.713128	5
GJ–35	Gui R.	690	138	31.3	87.4	84.9	1450	116	51.0		0.555	0.714357	8
GJ–36	Longjiang R.	78.5	74.1	33.8	106	47.4	270	48.6	56.5		0.124	0.724605	5
GJ–37	Gui R.										0.554	0.714018	5
GJ–38	Gui R.										0.516	0.714343	3
GJ–39	Siliang R.										0.361	0.720095	3
GJ–40	Gui R.										0.534	0.716453	4
Rain	Rain										0.110	0.710416	3

[a] Major ion concentrations in the Xishui River were from Wu et al. (2013). [b] Major ion concentrations in the Guijiang River were cited from Zhang et al. (2012b). Comparing with our samples, they were collected in different time (April 2012), and so can only be a reference.

HESSD

10, 8031–8069, 2013

Sr isotopic characteristics in small watersheds

W. H. Wu et al.

Discussion Paper | Discussion Paper | Discussion Paper | Discussion Paper |

Title Page

Abstract Introduction

Conclusions References

Tables Figures

◀◀ ▶▶

◀ ▶

Back Close

Full Screen / Esc

Printer-friendly Version

Interactive Discussion

Table 3. Sr isotopic compositions of the Xishui River and Guijiang River riverbed sediments and soils.

Num.	Sr (μg/g)	$^{87}Sr/^{86}Sr$	2σ
The Xishui River sediments			
XS-01	249	0.710139	2
XS-02	354	0.709188	3
XS-03	255	0.712616	3
XS-04	232	0.711184	4
XS-05	396	0.707058	3
XS-06	423	0.708789	4
XS-07	362	0.709222	3
XS-08	378	0.709050	4
XS-09	448	0.708784	3
The Guijiang River sediments			
GJ–01	41.6	0.743134	3
GJ–02	43.9	0.757536	4
GJ–03	56.6	0.738083	4
GJ–09	61.6	0.739180	3
GJ–10	54.6	0.742779	2
GJ–11	58.1	0.742161	4
GJ–15	49.1	0.744003	3
GJ–19	63.6	0.737776	3
GJ–20	47.8	0.758427	3
GJ–22	87.0	0.737306	4
GJ–23	77.3	0.737048	4
GJ–24	85.1	0.735172	3
GJ–25	93.8	0.735274	3
GJ–30	55.1	0.748129	4
GJ–31	59.6	0.740296	5
GJ–33	38.3	0.775952	4
GJ–34	52.2	0.761448	4
GJ–40	58.3	0.750115	4
The Guijiang River soils			
GJ–15	55.4	0.744095	5
GJ–19	48.3	0.749902	3

HESSD
10, 8031–8069, 2013

Sr isotopic characteristics in small watersheds

W. H. Wu et al.

Table 4. Sr isotopic compositions of underlying bedrocks in the Xishui River and Guijiang River catchments.

Lithologies	$^{87}Sr/^{86}Sr$	Data Source
The Xishui River catchment		
Granitoids	0.708229–0.716990	Ge et al. (2001a)
Granitoids	0.707934–0.713695	Chen et al. (2002)
Granitoids	0.707040–0.712890	Zhang et al. (2002)
Gray Gneisses	0.707482–0.719772	Zheng et al. (2000)
Pyroxenite/gabbro	0.706839–0.708556	Jahn et al. (1999)
Mafic-ultramafic Rocks	0.706071–0.703955	Li et al. (1998)
Eclogites	0.705388–0.710926	Liu et al. (2000)
Complex	0.707109–0.707611	Wawrzenitz et al. (2006)
Mafic igneous	0.707791–0.709900	Wang et al. (2005)
The Guijiang River catchment		
Granitoids	0.72261–0.99180	Zhu et al. (1989)
Granitoids	0.733000–1.025912	Gu et al. (2006)
Granitoids	0.738–1.003	Xu and Zhang (1993)
Granitoids	0.77007–0.89397	Xu et al. (1994)
Granitoids	0.720065–0.787221	Zhang et al. (2012a)
Carbonate rocks [a]	0.70589–0.70882	Huang (1997)
Carbonate rocks [a]	0.708223–0.708907	Zeng et al. (2007)
Dolomitic limestone [b]	0.70775	Liu et al. (2011)
Soil [b]	0.71049–0.72266	Liu et al. (2011)
Soil [b]	0.727317–0.727417	Zhu et al. (2011)

[a] Paleozoic carbonate rocks in the Yangtze Platform. [b] Karst area in the neighboring Guizhou Province.

HESSD
10, 8031–8069, 2013

Sr isotopic characteristics in small watersheds

W. H. Wu et al.

Table 5. Sr isotopic compositions of fertilizer, wastewater, groundwater, and plant in different land use patterns in karst area.

	Sr ($\mu g\, g^{-1}$)	$^{87}Sr/^{86}Sr$	Data Sources
Irrigation water	0.039	0.71234	Hosono et al. (2007)
Basal fertilizer	0.017–0.057	0.70827–0.70967	
Supplemental fertilizer	0.044–0.084	0.70894–0.71020	
Liquid fertilizer[a]	0.948	0.708078	Brenot et al. (2008)
Solid fertilizer	202	0.703313	
Winter sewage[a]	6.28–10.3	0.70804	Lang et al. (2006)
Summer sewage[a]	4.91–8.90	0.70800	
Industrial wastewater[a]	10.3	0.70766	Li et al. (2010)
Domestic wastewater[a]	4.57–5.02	0.70762–0.70820	
Farmland spring[a]	0.92–6.62	0.70794–0.70848	
Residential area spring[a]	1.26–4.45	0.70818–0.70835	
Cultivated land groundwater[a]	2.97–5.63	0.70814–0.71097	Jiang et al. (2009)
Grass land groundwater[a]	1.93–2.42	0.70758–0.70962	
Construction land groundwater[a]	3.71–7.63	0.70994–0.71089	
Forested land groundwater[a]	0.82–2.05	0.70778–0.70942	
Plants	4.9–222	0.70856–0.71145	Zheng et al. (2008)

[a] The unit of Sr concentrations is $\mu mol\, L^{-1}$.

Table 6. The contributions of different sources to Sr in the Xishui River solved by an inversion model.

	Atmospheric	Urban	Agriculture	Evaporite	Carbonate	Silicate
Winter	8.6–56.9 % (36.8 %)	0–0.4 % (0.1 %)	0	0–18.9 % (3.2 %)	8.4–28.7 % (18.7 %)	32.7–55.1 % (41.2 %)
Summer	0.8–25.4 % (19.5 %)	0–1.6 % (0.5 %)	0	6.5–15.7 % (11.4 %)	13.5–24.8 % (18.5 %)	42.2–69.4 % (50.1 %)

HESSD
10, 8031–8069, 2013

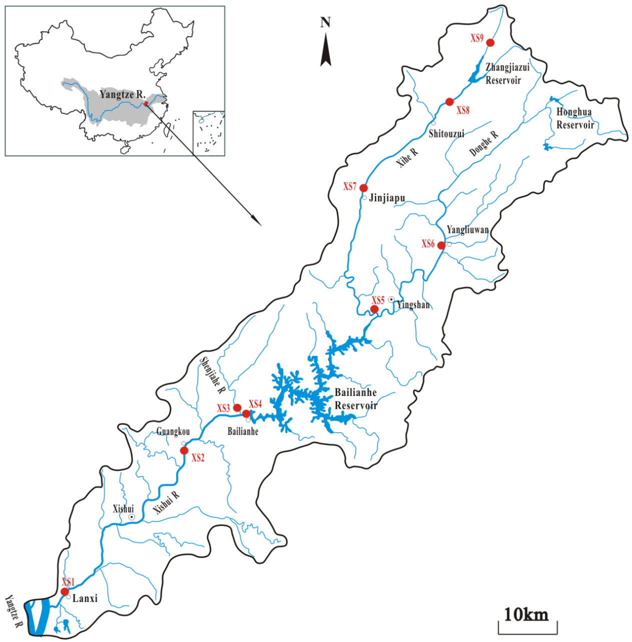

Fig. 1. Map of the Xishui River catchment and sampling locations (filled red circles).

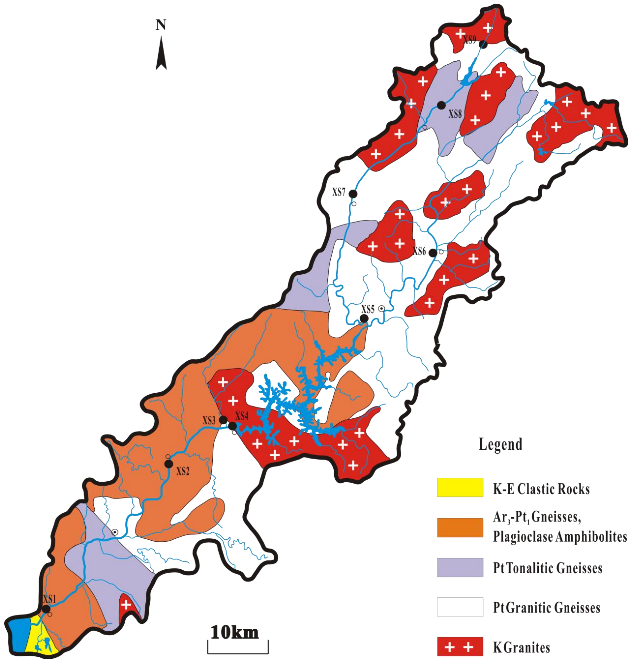

Fig. 2. Geological map of the Xishui River catchment (Modified from China Geological Survey, 2004).

HESSD
10, 8031–8069, 2013

Sr isotopic characteristics in small watersheds

W. H. Wu et al.

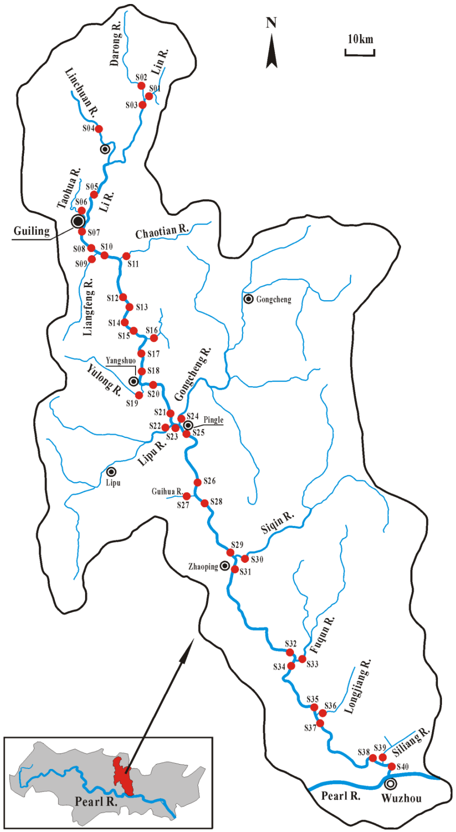

Fig. 3. Map of the Guijiang River catchment and sampling locations (filled red circles).

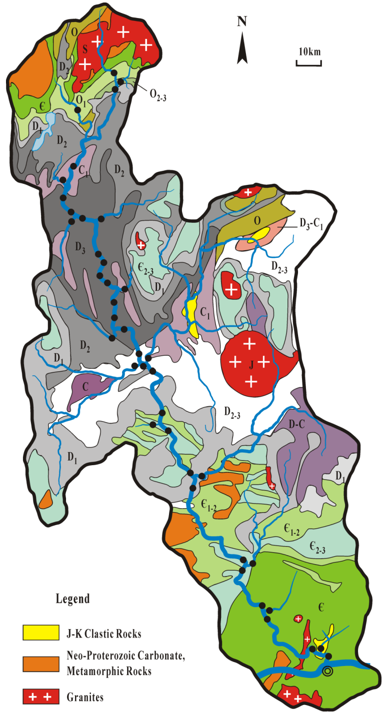

Fig. 4. Geological map of the Guijiang River catchment (Modified from China Geological Survey, 2004). E: Cambrian mixed-layer; E_{1-2}: limestones/dolomites intercalated shales; E_{2-3}: limestones intercalated shales; O: Ordovician mixed-layer; O_1: shales, mud rocks, limestones, and dolomites; D_1: sand rocks, mud rocks and few carbonate rocks; D_2: carbonate rocks and detrital rocks; D_{2-3}: carbonate rocks, sand rocks, and mud rocks; D_3: carbonate rocks; D_3–C_1: detrital rocks, carbonate rocks, and mud rocks; D–C: Devonian–Carboniferous mixed-layer; C: Carboniferous mixed-layer; C_1: carbonate rocks, sand rocks, and mud rocks intercalated coals.

HESSD
10, 8031–8069, 2013

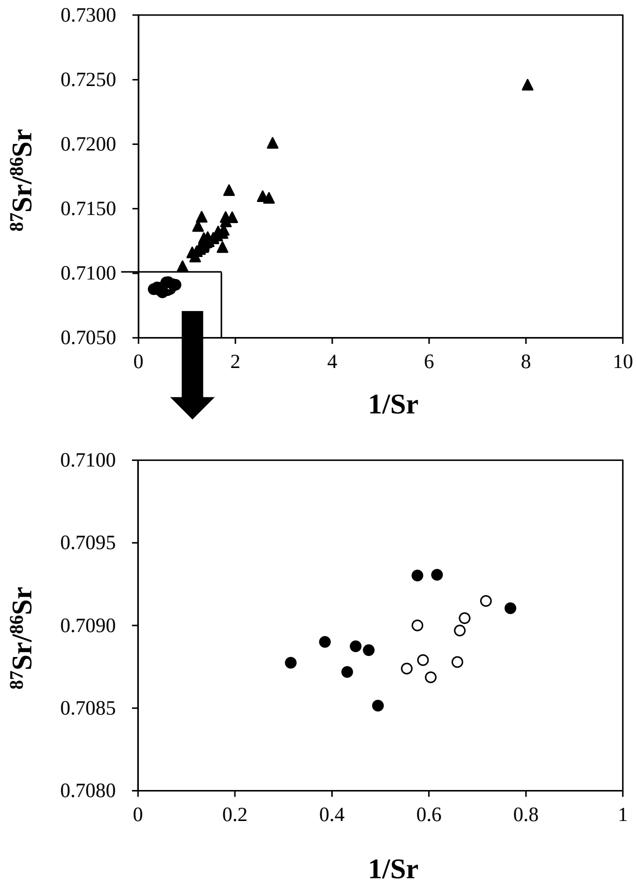

Fig. 5. A plot of $^{87}Sr/^{86}Sr$ vs. 1/Sr in the Xishui River and Guijiang River. The filled triangles are the samples in the Guijiang River, and the filled and open circles represent the samples in the Xishui River in winter and summer, respectively.

HESSD
10, 8031–8069, 2013

Sr isotopic characteristics in small watersheds

W. H. Wu et al.

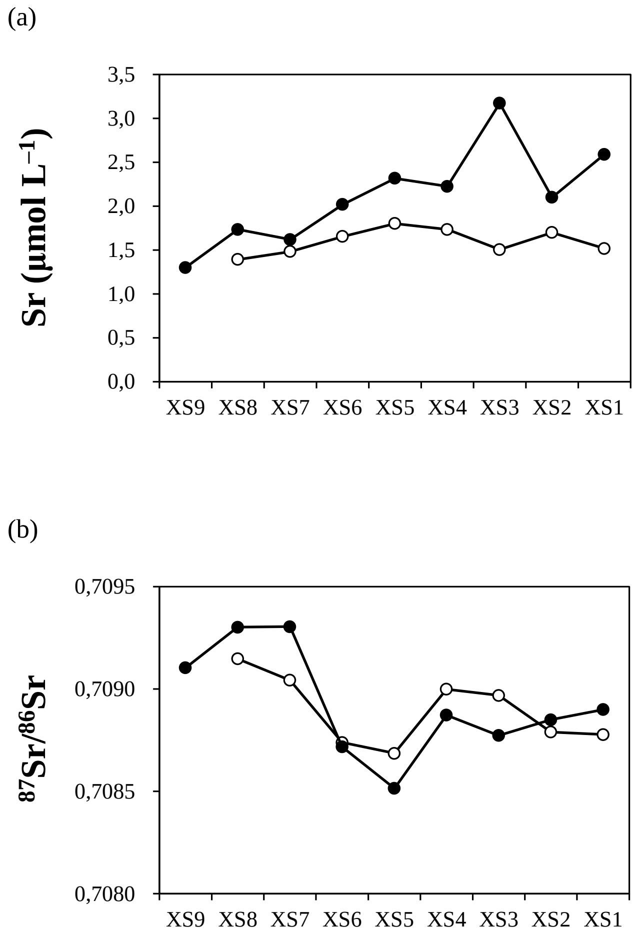

Fig. 6. Temporal and spatial variations of Sr concentrations **(a)** and $^{87}Sr/^{86}Sr$ ratios **(b)** in the Xishui River. The filled and open circles represent the samples in winter and summer, respectively.

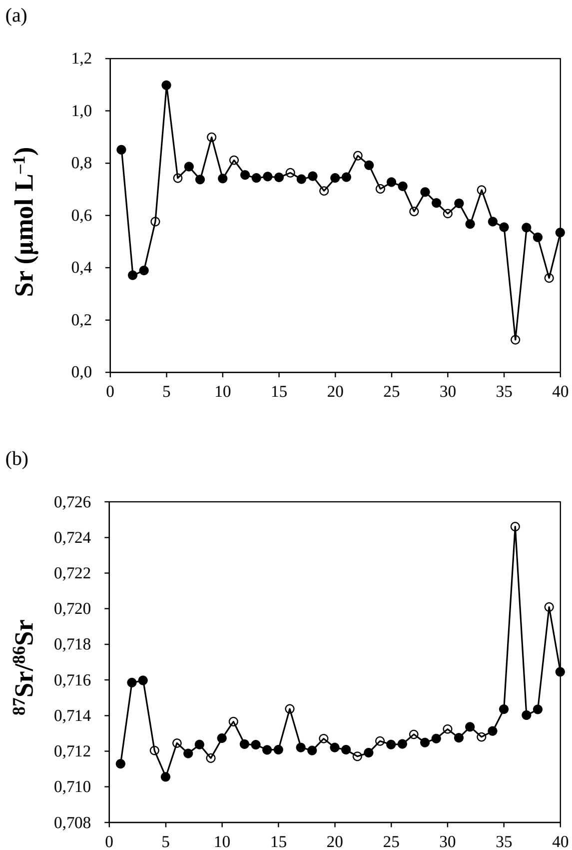

Fig. 7. Spatial variations of Sr concentrations **(a)** and $^{87}Sr/^{86}Sr$ ratios **(b)** in the Guijiang River. The filled and open circles represent the samples in the mainstreams and tributaries, respectively.

HESSD
10, 8031–8069, 2013

Title Page
Abstract | Introduction
Conclusions | References
Tables | Figures
◀| |▶
◀ ▶
Back | Close
Full Screen / Esc
Printer-friendly Version
Interactive Discussion